

**Natranaerofaba carboxydovora gen. nov., sp. nov., an extremely haloalkaliphilic CO-utilizing acetogen from a hypersaline soda lake representing a novel deep phylogenetic lineage in the class 'Natranaerobiia'**

Sorokin, Dmitry Y.; Diender, Martijn; Merkel, Alexander Y.; Koenen, Michel; Bale, Nicole J.; Pabst, Martin; Sissinghe Damsté, Jaap S.; Sousa, Diana Z.

**DOI**

[10.1111/1462-2920.15241](https://doi.org/10.1111/1462-2920.15241)

**Publication date**

2020

**Document Version**

Accepted author manuscript

**Published in**

Environmental Microbiology

**Citation (APA)**

Sorokin, D. Y., Diender, M., Merkel, A. Y., Koenen, M., Bale, N. J., Pabst, M., Sissinghe Damsté, J. S., & Sousa, D. Z. (2020). *Natranaerofaba carboxydovora* gen. nov., sp. nov., an extremely haloalkaliphilic CO-utilizing acetogen from a hypersaline soda lake representing a novel deep phylogenetic lineage in the class 'Natranaerobiia'. *Environmental Microbiology*, 23(7), 3460-3476. <https://doi.org/10.1111/1462-2920.15241>

**Important note**

To cite this publication, please use the final published version (if applicable).  
Please check the document version above.

**Copyright**

Other than for strictly personal use, it is not permitted to download, forward or distribute the text or part of it, without the consent of the author(s) and/or copyright holder(s), unless the work is under an open content license such as Creative Commons.

**Takedown policy**

Please contact us and provide details if you believe this document breaches copyrights.  
We will remove access to the work immediately and investigate your claim.



***Natranaerofaba carboxydovora* gen. nov., sp. nov., an extremely haloalkaliphilic CO-utilizing acetogen from a hypersaline soda lake representing a novel deep phylogenetic lineage in the class "*Natranaerobiia*"**

Journal:	<i>Environmental Microbiology and Environmental Microbiology Reports</i>
Manuscript ID	EMI-2020-1271.R2
Journal:	Environmental Microbiology
Manuscript Type:	EMI - Special Issue Article
Date Submitted by the Author:	n/a
Complete List of Authors:	Sorokin, Dmitry; Winogradsky Institute of Microbiology RAS, ; TU Delft, Biotechnology Diender, Martijn; Wageningen Universiteit en Research, Microbiology and Ecosystem Science Merkel, Alexander; Winogradsky INMI RAS, Lab. hyperthermophilic microbial communities Koenen, Michel; NIOZ Bale, Nicole; Royal Netherlands Institute for Sea Research, Marine Organic Biogeochemistry Damsté, Jaap Sousa, Diana; Wageningen University, Laboratory of Microbiology; Pabst, Martin; Delft University of Technology Department Biotechnology, Biotechnology
Keywords:	soda lake, haloalkaliphilic, carboxydotrophic, " <i>Natranaerobiia</i> ", acetogen

SCHOLARONE™  
Manuscripts

1 ***Natranaerofaba carboxydovora* gen. nov., sp. nov., an extremely**  
2 **haloalkaliphilic CO-utilizing acetogen from a hypersaline soda lake**  
3 **representing a novel deep phylogenetic lineage in the class**  
4 **"*Natranaerobiia*"**

5  
6 *Dimitry Y. Sorokin*<sup>1,2\*</sup>, *Martijn Diender*<sup>3</sup>, *Alexander Y. Merkel*<sup>1</sup>, *Michel Koenen*<sup>4</sup>, *Nicole J.*  
7 *Bale*<sup>4</sup>, *Martin Pabst*<sup>2</sup>, *Jaap S. Sinninghe Damsté*<sup>4,5</sup>, and *Diana Z. Sousa*<sup>3</sup>  
8

9 <sup>1</sup>*Winogradsky Institute of Microbiology, Research Centre of Biotechnology, Russian Academy of Sciences,*  
10 *Moscow, Russia*

11 <sup>2</sup>*Department of Biotechnology, Delft University of Technology, Delft, The Netherlands*

12 <sup>3</sup>*Laboratory of Microbiology, Wageningen University, Wageningen, The Netherlands*

13 <sup>4</sup>*NIOZ Royal Netherlands Institute for Sea Research, Department of Marine Microbiology and Biogeochemistry,*  
14 *and Utrecht University, Den Burg, The Netherlands.*

15 <sup>5</sup> *Department of Geosciences, Utrecht University, Utrecht, The Netherlands*  
16

17 \*Correspondence: Dimitry Sorokin (soroc@inmi.ru; d.sorokin@tudelft.nl)  
18  
19

20 **Originality-Significance Statement**

21 This paper describes the first example of an extremely haloalkaliphilic anaerobic bacterium  
22 isolated from a hypersaline soda lake capable of CO utilization as electron donor. It represents  
23 a member of a novel deep-branching phylogenetic lineage at the level of a new genus and  
24 family within the Firmicutes class "*Natranaerobiia*". Based on its basic physiology, the  
25 bacterium is an acetogen with a restricted metabolism capable of anaerobic respiration with  
26 thiosulfate and nitrate.

## 1 **Summary**

2 An anaerobic enrichment with CO from sediments of hypersaline soda lakes resulted in a  
3 methane-forming binary culture, whereby CO was utilized by a bacterium and not the  
4 methanogenic partner. The bacterial isolate ANCO1 forms a deep-branching phylogenetic  
5 lineage at the level of a new family within the class "*Natranaerobiiia*". It is an extreme  
6 haloalkaliphilic and moderate thermophilic acetogen utilizing CO, formate, pyruvate and  
7 lactate as electron donors and thiosulfate, nitrate (reduced to ammonia) and fumarate as  
8 electron acceptors. The genome of ANCO1 encodes a full Wood-Ljungdahl pathway allowing  
9 for CO oxidation and acetogenic conversion of pyruvate. A locus encoding Nap nitrate  
10 reductase/NrfA ammonifying nitrite reductase is also present. Thiosulfate respiration is  
11 encoded by a Phs/Psr-like operon. The organism obviously relies on Na-based bioenergetics,  
12 since the genome encodes for the Na<sup>+</sup>-Rnf complex, Na<sup>+</sup>-F1F0 ATPase and Na<sup>+</sup>-translocating  
13 decarboxylase. Glycine betaine serves as a compatible solute. ANCO1 has an unusual  
14 membrane polar lipid composition dominated by diethers, more common among archaea,  
15 probably a result of adaptation to multiple extremophilic conditions. Overall, ANCO1  
16 represents a unique example of a triple extremophilic CO-oxidizing anaerobe and is classified  
17 as a novel genus and species *Natranaerofaba carboxydovora* in a novel family  
18 *Natranaerofabacea*.

19  
20 Key words: **soda lake, haloalkaliphilic, carboxydophilic, acetogen, "*Natranaerobiiia*"**

## 1 **Introduction**

2 In view of the possibility of an early soda ocean (created by CO<sub>2</sub> weathering of Na/K-rich  
3 basalt crust of volcanic origin) in the geological history of Earth and Mars and a probability of  
4 the same in the current ocean on Europa, there is an interest in astrobiology of the existing  
5 haloalkaline environments on Earth, such as terrestrial soda lakes and deep sea  
6 serpentinization area (Fox-Pawel *et al.*, 2016; Herschy *et al.*, 2014; Kempe and Kazmierczak,  
7 2002). One of the potential common substrates for extraterrestrial microbes would be CO,  
8 which can form by photolysis of CO<sub>2</sub> under strong UV radiation (King, 2015).

9 Modern saline-alkaline soda lakes represent rare examples of stable highly alkaline  
10 natural habitats due to the presence of high concentrations of soluble sodium carbonates,  
11 which can reach molar concentrations in hypersaline soda lakes. Such lakes are located in arid  
12 areas characterized by a hot climate with long periods of evaporative salt concentration  
13 (Schagerl, 2016). Thus, prokaryotes thriving in soda lakes often exhibit triple extremophilic  
14 circumstances, i.e. halo-alkalo-thermo-phily (Mesbah *et al.* 2007; 2009; Sorokin *et al.*, 2017).

15 Extensive knowledge has been accumulated in the past three decades on the  
16 functionally important microbial communities in soda lakes, both by culture-dependent (Grant  
17 and Jones, 2016; Sorokin *et al.*, 2015; Sorokin, 2017) and culture-independent molecular  
18 approaches (Vauvorakis *et al.*, 2017; 2019; Zorz *et al.*, 2019). However, several pieces of the  
19 puzzle are still missing. In particular, whether anaerobic carbon monoxide oxidation  
20 (carboxydrotrophy) is possible under extremely haloalkaline conditions. Aerobic  
21 carboxydrotrophy has been shown for a group of highly salt tolerant soda lake alkaliphiles  
22 belonging to two closely related genera *Alkalispirillum/Alkalilimnicola* of the  
23 *Gammaproteobacteria* (Hoeft *et al.*, 2007; Sorokin *et al.*, 2010). The only anaerobic isolate  
24 reported as capable of CO oxidation at high pH is the acetogenic *Alkalibaculum bacchii*, a

1 nonhalophilic, alkalitolerant member of the *Eubacteriaceae* family (*Firmicutes*), isolated  
2 from soil (Allin *et al.*, 2010; Liu *et al.*, 2012).

3 Three major types of anaerobic carboxydrophy have been established: by acetogens  
4 via the Wood-Ljungdahl pathway, resulting in CO<sub>2</sub>, acetate and/or ethanol; by methanogens,  
5 resulting in methane or acetate; and by hydrogenogens, resulting in H<sub>2</sub> and CO<sub>2</sub> (Diender *et*  
6 *al.*, 2015). Since protons are the final electron acceptors of hydrogenogens, the  
7 hydrogenogenic metabolism is highly improbable under soda lake conditions, while both  
8 acetogenic and methanogenic CO utilization are possible. There is a fourth (marginal)  
9 pathway of anaerobic carboxydrophy, the direct anaerobic oxidation of CO in presence of a  
10 suitable electron acceptor, but it has not yet been well studied, except for sulfate-reducing  
11 conditions, exemplified by *Desulfotomaculum* species (Parshina *et al.*, 2010) and  
12 *Archaeoglobus fulgidus* (Henstra *et al.*, 2007).

13 Our previous attempts to directly enrich either acetogenic or methanogenic CO-  
14 utilizing haloalkaliphiles from soda lakes at mesophilic conditions and low salinity (0.6 M  
15 total Na<sup>+</sup>, pH 10, 30°C and 0.2 atm CO in the gas phase) resulted in a positive acetogenic  
16 enrichment consisting of five clostridia members distantly related to the genera *Anaerobranca*  
17 and *Dethiobacter*. However, efforts to further enrich the consortium failed and the culture was  
18 eventually lost. Recently, another trial was undertaken to find out whether CO could replace  
19 formate/H<sub>2</sub> as the electron donor for triple extremophilic methyl-reducing methanogens of the  
20 class *Methanonatronarchaeia* found in hypersaline soda lakes (Sorokin *et al.*, 2017; 2018).  
21 Methane was indeed formed in such enrichments but not directly by methanogens. Instead, a  
22 triple extremophilic anaerobic bacterium capable of utilizing CO as the electron donor was  
23 responsible for the initial CO conversion. Its phenotypic, phylogenetic and genomic  
24 properties are described in this paper.

25

26

## 1 RESULTS

2

### 3 **Enrichment and isolation of a haloalkaliphilic carboxydrotrophic bacterium**

4 In the primary enrichment, inoculated with anaerobic sediment from a hypersaline soda lake,  
5 methane formation at 50 °C in presence of CO/MeOH as substrates was only observed at the  
6 minimal CO concentration of 0.05 atm in the gas phase. The onset of methane accumulation  
7 occurred after a prolonged lag period (0.3% in the gas phase after 53 d) and reached a  
8 maximum of 3.2% at day 85. Interestingly, all CO had already been consumed at day 65,  
9 indicating that the CO consumption and methane formation were not synchronized. However,  
10 no methane formation occurred in control incubations lacking CO. In the second 1:100  
11 transfer of this culture, two major cell morphotypes were observed: bean-shaped motile cells  
12 and tiny angular cocci typical for the genus *Methanonatronarchaeum*. This assumption was  
13 later confirmed by isolating this methyl-reducing methanogen from the consortium using  
14 formate instead of CO as the electron donor. It had 100% 16S-rRNA gene identity to one of  
15 the previously isolated strain of *M. thermophilum* (Sorokin *et al.*, 2017; 2018) and it was  
16 unable to use CO as the electron donor in pure culture. Therefore, it was concluded that the  
17 bean-shaped bacterium was the primary CO-utilizing organism in this consortium, which  
18 might have converted part of CO into formate utilized by the methyl-reducing methanogen.  
19 The CO-utilizing bacterium was finally separated from the methanogen in serial dilutions  
20 using higher CO concentration (10-20% in the gas phase) and omitting MeOH from the  
21 medium. Furthermore, we repeated the enrichment at these modified conditions with the  
22 inoculum diluted from the start and the same bacterium was selected up to a 10<sup>-8</sup> dilution,  
23 indicating that this was the only carboxydrotrophic anaerobe capable of growing at the used  
24 triple extremophilic conditions. The isolated pure culture strain was designated ANCO1.

25

## 1 **Phylogeny of strain ANCO1**

2           The 16S rRNA-based phylogenetic analysis placed strain ANCO1 into the *Firmicutes*  
3 order *Natranaerobiales* (elevated to the level of a class "*Natranaerobiia*" according to the  
4 phylogenomic taxonomy, <https://gtdb.ecogenomic.org>) as a deep-branching lineage (**Fig. 1a**).  
5 The closest relative of ANCO1 (90% sequence identity) is the moderately salt-tolerant  
6 alkaliphilic peptidolytic anaerobe *Natranaerobaculum magadiense*, isolated from hypersaline  
7 soda lake Magadi in Kenya (Zavarzina *et al.*, 2013). A more advanced phylogenomic analysis  
8 based on 120 conserved single copy marker genes confirmed the independent position of  
9 strain ANCO1 within the class "*Natranaerobiia*" at the level of a new family (**Fig. 1b**): the  
10 relative evolutionary divergence (RED) value of the node of *N. carboxydovora* offshoot  
11 calculated using GTDBtk was 0.663 (values of 0.773 and 0.629 considered as family and  
12 order thresholds, respectively) (Parks *et al.* 2018). AAI values between ANCO1 and members  
13 of the type genus *Natranaerobius* did not exceed 48%.

14

## 15 **Cell morphology**

16           ANCO1 has bean-shaped cells of variable length, from 2 to 5  $\mu\text{m}$ , depending on the  
17 growth rate, motile with a few flagella located on the concave side of the cell (**Fig. 2**).  
18 Although endospore formation was not observed at the growth conditions used, the genome  
19 does contain several extended loci encoding this capacity.

20

## 21 **Membrane polar lipids**

22           ANCO1 contains a wide range of intact polar lipids (IPLs) (**Table 2**). These all had  
23 either a phosphocholine (PC) or phosphoglycerol (PG) polar head group and the PCs were  
24 dominant over the PGs. The apolar cores of the IPLs comprised a distinctive range of  
25 different structures. The alkyl chains (containing between 14 and 19 carbon atoms) were



1 bound to the glycerol backbone via either ester or ether bonds giving rise to diacyl lipids (two  
2 ester bonded chains), diether lipids and mixed acyl/ether lipids (including plasmalogen  
3 lipids). Mixed acyl/ether lipids have been reported in anaerobic bacteria, with some  
4 exceptions in aerobic bacteria, and are thought to improve cell resistance to extreme external  
5 conditions (Grossi *et al.*, 2015). The majority ( $\leq 80\%$ ) of the lipids in ANCO1 were diethers,  
6 which are rare in bacteria but are characteristic of archaeal membranes. A number of the  
7 bacterial species that have been reported to produce diether lipids belong to thermophiles (e.g.  
8 Langworthy *et al.*, 1983; Huber *et al.*, 1992; Hamilton-Brehm *et al.*, 2013). Macrocylic  
9 diethers were also detected in ANCO1 as a minor component. These have not previously been  
10 described in pure bacterial cultures but have been detected in environments including  
11 authigenic carbonates from marine evaporites, probably formed at high temperatures and high  
12 salinity (Baudrand *et al.*, 2010; Ziegenbalg *et al.*, 2012), iron sulfide nodules formed during  
13 the anaerobic oxidation of methane (van Dongen *et al.*, 2007), geothermal hot springs  
14 (Pancost *et al.*, 2006) and iron sulfides from a Mid-Atlantic hydrothermal field (Blumenberg  
15 *et al.*, 2007). The archaeal equivalent of this lipid, an isoprenoidal macrocylic diether  
16 (known as macrocylic archaeol) has been shown to augment membrane impermeability and  
17 stability in thermophilic methanogenic archaea (Koga *et al.*, 1998), which explains its  
18 accumulation in extremophilic archaea (Sprott *et al.*, 1991; Bale *et al.*, 2019b).

19 The individual constituents of the core lipids were also analyzed directly in more  
20 detail, after hydrolysis of the biomass to cleave off the polar head groups (see Supplementary  
21 **Fig. S2** for examples of structures and theoretical hydrolysis schemes). This procedure  
22 released fatty acids (FA; formed from ester bound alkyl chains), dimethyl acetals [DA;  
23 formed from plasmalogen lipids; van Gelder *et al.* (2014)] and mono and dialkyl glycerol  
24 ethers (MGEs and DGEs; formed from ether-bound alkyl chains). Both straight-chain and  
25 branched alkyl chains were present. As the DGEs contain two alkyl chains (Supplementary

1 **Fig. S2**), their total number of alkyl carbon atoms range between 29 and 34. Overall  
2 conclusion of the lipid analysis is that its unusual composition most probably reflects the  
3 triple extremophilic nature of strain ANCO1.

4 The respiratory lipoquinoines were not detectable in ANCO1, either because they were  
5 present at a very low level or because they are not produced. The latter is likely since the  
6 genome does not contain the genes encoding the enzymes required for menaquinone  
7 biosynthesis.

### 9 **Growth physiology of strain ANCO1**

10 Growth with CO as the electron donor (and other electron donors) was only possible in  
11 the presence of at least 100 mg/l of yeast extract. After gradual adaptation, ANCO1 was able  
12 to tolerate up to 50% CO in the gas phase. However, the maximum biomass yield reached  
13 only 10 mg cell protein l<sup>-1</sup> even at highest CO concentration, and the full CO consumption  
14 was observed only at 5-10% CO. The only gaseous product detected was CO<sub>2</sub>, although most  
15 of it was apparently absorbed into the highly alkaline culture medium (**Supplementary Fig.**  
16 **S1**). Liquid analysis at the end point in the incubation with 5% CO (11.5 mM) showed  
17 formation of two organic products - acetate as a major and formate as a minor component (2.5  
18 and 0.8 mM, respectively), indicating that the mode of anaerobic CO conversion in ANCO1 is  
19 homoacetogenic (4 mol CO > 1 mol acetate). Both formate and acetate can be utilized by  
20 *Methanonatroarchaeum* (as electron donor and C-source, respectively) which might explain  
21 why the initial enrichment supported growth of this methyl-reducing methanogen.

22 An enzymatic assay confirmed the presence of anaerobic CODH activity in strain  
23 ANCO1 (1.77 ± 0.22 μmol/min of CO conversion per mg protein in cell free extract). The  
24 only another compound supporting acetogenic growth from a range of substrates tested (H<sub>2</sub>,

1 formate, MeOH, EtOH, PrOH, BuOH, lactate, and sugars) was pyruvate, which was  
2 converted into acetate and lactate with a minor formation of H<sub>2</sub> (0.2-0.3 mM).

3 The ability of ANCO1 to use various electron acceptors was first tested with the two  
4 positive electron donors, i.e. CO and pyruvate. A definite growth stimulation was observed  
5 with fumarate and thiosulfate. The latter was partially reduced to sulfite and sulfide, while  
6 succinate formation from fumarate was very weak, which is difficult to explain, especially  
7 because fumarate reductase genes are present in the genome (**Table 1**).

8 The genomic data (see below) suggested that ANCO1 has a potential for dissimilatory  
9 reduction of nitrate to ammonia (DNRA). However, tests with CO and pyruvate showed  
10 neither growth stimulation nor nitrate (5 mM) consumption, and addition of even 2 mM nitrite  
11 inhibited growth. Therefore, other potential electron donors (suggested by the genome  
12 composition) were tested: formate, H<sub>2</sub> and lactate. The latter two were negative, while  
13 anaerobic growth with formate as the electron donor was possible with thiosulfate, fumarate  
14 and nitrate/nitrite. The ammonifying growth of ANCO1 was not easy to prove. When nitrate  
15 was added at 5 mM from the start, it was converted only to nitrite. At 2 mM initial  
16 concentration, however, ammonifying growth with formate as donor was possible up to two  
17 further additions of 2 mM portions of nitrate. In total, 6 mM of nitrate were consumed without  
18 formation of intermediate nitrite and 4 mM NH<sub>3</sub> was detected in the end of incubation. Nitrite  
19 could also support ammonifying growth with formate, but only when it was added at low  
20 concentration of 2 mM together with formate (50 mM) to a culture, pre-grown with pyruvate  
21 or to a culture started to grow with formate + fumarate. It was possible to add in total up to 6  
22 mM nitrite in three portions and the final ammonia production reached 5.3 mM with a  
23 prominent biomass increase in comparison to the control without nitrite addition. A direct  
24 addition of even 2 mM nitrite to the formate culture from the start revealed the complete  
25 absence of growth. Furthermore, formate was the only electron donor for which significant

1 amount of succinate was detected during growth with fumarate as the electron acceptor. On  
2 the other hand, sulfidogenic growth on formate with thiosulfate produced the least sulfide  
3 from other positive cases (**Table 1**).

4 Lactate as the potential electron donor was also tested with fumarate and thiosulfate as  
5 the electron acceptors. In both cases growth was observed, with very active sulfide formation  
6 from thiosulfate, but only trace amount of succinate was formed during growth with fumarate.  
7 No growth was detected with H<sub>2</sub> at any tested conditions (**Table 1**).

8 Influence of salt and pH on growth of ANCO1 was tested with pyruvate +fumarate.  
9 Both profiles showed growth only at a limited range, indicating an extreme specialization of  
10 this organism to live in hypersaline soda lake conditions (**Fig. 3**). The salt profile (obtained at  
11 pH 9.5) showed that ANCO1 is an extreme halophile, growing within a range of total Na<sup>+</sup>  
12 from 2.5 to 4.5 M (optimum at 4 M). It is an obligate alkaliphile, growing within a narrow pH  
13 range above 9 and up to 10.5 (optimum at 9.5; the final pH measured at 30 °C). On its  
14 temperature dependence, ANCO1 can be qualified as a moderate thermophile with the growth  
15 range from 35 to 56 °C and an optimum at 48-50 °C.

16

### 17 **Functional genomic and proteomic analyses**

18 The genome of ANCO1 (accession number CP054394) was assembled into a single  
19 contig of 3.26 MB, which is predicted to be circular and has a GC content of 35.3 mol%.  
20 Plasmids were not detected. Annotation produced 3,120 coding sequences. The key functional  
21 pathways found in the genome of ANCO1 are summarized in **Figure 4** and the identified  
22 genes/proteins are listed in the **Supplementary Table S1**. The key expressed functional  
23 proteins are shown on **Supplementary Fig. S3** and listed in **Supplementary Table S2**. The  
24 full range of expressed proteins is provided in the **Extended proteomic data file**.

1           The ANCO1 genome contains all the genes of the Wood-Ljungdahl pathway and  
2 corresponding enzymes were indeed detected in the proteome of ANCO1 grown on CO and  
3 pyruvate. The presence of three CODH-encoding genes in the genome and the detection of  
4 CODH activity in cell free extracts confirms the ability of the bacterium to utilize CO as  
5 electron donor. ANCO1 encodes for one CODH/ACS cluster, likely involved in CO-oxidation  
6 as well as CO<sub>2</sub> fixation. When the organization of this gene cluster is compared to  
7 corresponding CODH/ACS clusters of other carboxydophilic genomes, most similarity is  
8 observed with the thermophilic acetogens *Moorella thermoacetica* and *Carboxydotherrmus*  
9 *hydrogeniformans* (**Figure 5**). Next to a CODH/ACS cluster, ANCO1 encodes for two other  
10 CODHs that are likely monofunctional. One lies adjacent to a hydrogenase complex  
11 (ACONDI\_01147-1151). However, carboxydophilic hydrogenogenic activity was not  
12 apparent from the physiological tests (no H<sub>2</sub> formation from CO), which means that this  
13 hydrogenase is not linked with the CODH, like, for example, Ech is.

14           The annotated cytoplasmic Fe-only hydrogenases exhibit similarity to bifurcating  
15 NADPH-dependent hydrogenases potentially involved in redox distribution, in particular to  
16 recycle NAD(P)H and ferredoxin pools used as reductants for biosynthesis, building  
17 membrane potential and anaerobic respiration (Buckel and Thauer, 2013). Several formate  
18 dehydrogenases are also present, of which two (ACONDI 00243-00246 and 02919-02924)  
19 show similarity with the CO-reactive hydrogenase of *Acetobacterium woodii* (HDCR type,  
20 Schuchmann et al., 2013), and may be used to link hydrogen oxidation to formate production.  
21 Genes encoding acetate kinase and acetyl-phosphotransferase are present, enabling acetate  
22 production from acetyl-CoA and energy conservation.

23           Comparative proteomic analysis of cells grown acetogenically either with CO or  
24 pyruvate was performed in order to understand more about the CO-specific metabolism of  
25 ANCO1. However, it appears, that the same set of enzymes involved mostly in the Wood-

1 Ljungdahl pathway and pyruvate oxidation were equally expressed (Supplementary **Fig. S3**  
2 **and Table S2**). This might indicate that both CO and pyruvate are funneled into the same  
3 pathway.

4       Regarding key energy-related reactions, ANCO1 encodes for a Rnf-complex and F1F0  
5 ATP synthase (both annotated as sodium-translocating). In addition, two membrane bound  
6 primary sodium-translocating decarboxylases are present: glutaconyl-CoA and  
7 methylmalonyl-CoA decarboxylase, which are potentially involved in the sodium-based  
8 bioenergetics and a control of sodium levels and osmoregulation in anaerobic alkaliphiles  
9 (Buckel, 2001; Dimroth and Schink, 1998). Further fate of the thioester products (propionyl-  
10 CoA and crotonyl-CoA) of these two putative reactions is difficult to predict, but, likely, they  
11 might be channeled into anabolic routes, such as amino acid or lipid biosynthesis.

12       Several proton/sodium antiporters are also encoded, including two multi-subunit Mnh  
13 complexes, one independent (ACONDI 02179-02187) and another one in a large locus  
14 together with the Na<sup>+</sup>-Rnf complex (ACONDI 00389-00396), enabling linkage of the proton  
15 and sodium gradients and maintenance of pH homeostasis. Also, a secondary sodium pump -  
16 potassium-stimulated Na<sup>+</sup>-pyrophosphatase, involved the ATP-dependent Na<sup>+</sup> removal from  
17 the cytoplasm is encoded by ACONDI 00187.

18       For osmoprotection, the genome predicts two potential pathways of glycine betaine  
19 biosynthesis. The first is sequential glycine methylation (ACONDI 00109/00157), including  
20 glycine/sarcosine and sarcosine/*N,N*-dimethylglycine methyltransferases (Roberts, 2005). The  
21 second is the oxidative pathway from carnitin (ACONDI 01812/01814), including L-  
22 carnithine dehydrogenase LcdH and 3-keto-5-aminohexanoate cleavage enzyme Kce  
23 (Rebouche, 1998). In addition, a presence in the ANCO1 genome of genes coding for  
24 multiple types of transporters for betaine/carnitin/choline import (Angelidis and Smith, 2003;  
25 Ongagna-Yhombi et al., 2015; Pflüger and Müller, 2004) strongly suggest that active

1 transport of betaine and its precursors is active in the ANCO1 as well. These include the  
2 following families: BCCT, Gbu, BetS, OpuAC, OpuAB, OpuE and OpuD (the full list with  
3 the locus tags is present in **Supplementary Table S1**). A possible source of betaine for  
4 import might be yeast extract required by ANCO1 for growth at any conditions. Furthermore,  
5 potassium may play a significant role in osmoprotection too, judging from the presence of a  
6 large repertoire of genes encoding potassium import/export (KefC, TrkA, TrkAH, KtrAB,  
7 NhaP2, Kch) (**Supplementary Table S1**). Calculation of the total proteome acidity using the  
8 IPC calculator (<http://isoelectric.org/calculate.php>) showed a bimodal distribution of the pI  
9 value, with a major moderately acidic peak between pH 4 and 6 and a smaller basic peak  
10 between pH 8 and 10 (**Supplementary Fig. S4**), indicating that ANCO1 is most probably  
11 using the "salt-out" strategy as the dominant osmoprotection mechanism with potassium  
12 import as a secondary mechanism. But for the definite conclusion, both intracellular betaine  
13 and potassium accumulation needs to be determined.

14 Despite the inability to grow on sugars, the genome of ANCO1 encodes for the  
15 complete pentose-phosphate pathway and glycolysis. However, it lacks sugar transporters,  
16 suggesting that these pathways are most likely used for gluconeogenesis. Presence of  
17 pyruvate oxidoreductase enables conversion of acetyl-CoA into pyruvate for assimilatory  
18 metabolism. An incomplete TCA-cycle lacking malate dehydrogenase is encoded by the  
19 genome of ANCO1.

20 Despite the absence of lipoquinones (both by direct analysis and predicted by the lack  
21 of genes encoding menaquinone biosynthesis), the genome analysis confirms the potential of  
22 ANCO1 to obtain energy by nitrate/nitrite ammonification and thiosulfate- and fumarate-  
23 dependent respiration found in growth experiments. For DNRA, ANCO1 potentially uses an  
24 unusual module encoded in a single locus consisting of an intracellular truncated Nap type  
25 respiratory nitrate reductase NapAGHDF (ACONDI 01139-01143) and an exported

1 ammonifying nitrite reductase NrfA (ACONDI 01136). The locus, however, appears to lack  
2 NrfH, a membrane tetraheme *c* involved in electron transport to NrfA from quinones. As the  
3 NrfA present in the genome is predicted to have a single transmembrane helix and lies in the  
4 same operon as the Nap nitrate reductase, this might indicate a possibility for direct electron  
5 transfer from a membrane electron donor (which is still unknown) and an interaction between  
6 the two complexes. On the other hand, the genome also contains another locus that encodes a  
7 mosaic redox complex with an uncertain (to predict) function (ACONDI 02948-  
8 02952/02956). It includes a membrane diheme  $b_{556}$  cytochrome of the PhsC/NarI type (might  
9 be a missing subunit of the Phs operon, see below), followed by a putative NarG (catalytic  
10 subunit of the membrane respiratory nitrate reductase). Next, a tetraheme *c* cytochrome of the  
11 NapC/CymA type containing a single transmembrane loop is encoded. While not homologous  
12 to the integral membrane NrfH, it still might potentially be involved in the DNRA of ANCO1.  
13 The last part of this locus codes for the electron transfer complex FixXCA.

14       The genome of ANCO1 includes an operon coding for PhsAB complex (both subunits  
15 are exported) potentially involved in a 2-electron reduction of thiosulfate, but apparently  
16 lacking its membrane electron-transferring anchor PhsC, which might be encoded in another  
17 genomic locus (see above). Subunits of fumarate reductase (FrdAB) potentially involved in  
18 fumarate respiration are also present. A membrane associated NADPH oxidoreductases and a  
19 formate dehydrogenase (ACONDI-00243-00246) might be involved in donation of electrons  
20 to the respiration metabolism. However, the absence of respiratory lipoquinones still  
21 questions how those are linked to the electron-accepting respiratory complexes. The only  
22 candidate for the electron transfer encoded in the genome is a low-potential diheme *c* split-  
23 Soret cytochrome (ACONDI-02684), which is exported and attached to membrane. Such  
24 cytochromes serve in electron transport of sulfate-reducing bacteria (Devreese et al., 1997).



1 Despite the observed lactate production and utilization by the strain, lactate  
2 dehydrogenase could not be clearly annotated. However, the genome encodes for an operon  
3 encoding for a bifurcating lactate dehydrogenase, similar to an earlier reported bifurcating  
4 lactate dehydrogenase complex (Weghoff et al., 2014). This complex might be involved in the  
5 utilization of lactate for respiration and could additionally be involved in lactate production  
6 when grown on pyruvate, which is in line with the proteomics data showed relatively high  
7 abundance of this complex in cell grown on pyruvate.

8

## 9 DISCUSSION

10

11 Strain ANCO1 represents the first example of an extremely haloalkaliphilic CO-utilizing  
12 anaerobe. It is a member of a deep-branching phylogenetic lineage in the phylum *Firmicutes*,  
13 class "*Natraanaerobiiia*", which currently consists of only three genera found in soda lakes:  
14 the extremely salt-tolerant genera *Natranaerobius* and *Natronovirga* (Mesbah et al., 2007;  
15 Mesbah and Wiegel, 2009) and a moderately salt-tolerant genus *Natranaerobaculum*  
16 (Zavarzina et al., 2013). All of them are moderately thermophilic, obligately anaerobic  
17 fermentative heterotrophs with potential for anaerobic respiration, and in these the new  
18 member of this branch, strain ANCO1, is most similar to *Natranaerobius thermophilus*,  
19 which is also evident from the genome analysis (see **Supplementary Table S1**). However,  
20 the ability to utilize CO as electron donor has not been reported for any of the ANCO1  
21 relatives and the available genomes from the *Natranaerobius* species lack the respective  
22 genetic potential for such metabolism. The CODH/ACS cluster in ANCO1 is similar to that of  
23 other thermophilic carboxydrotrophs, like *Moorella thermoacetica* and *Carboxydotherrmus*  
24 *hydrogenoformans* (**Figure 5**). The main product of CO conversion by strain ANCO1 is  
25 acetate, similar to what is observed in *M. thermoacetica* (Drake and Daniel, 2004).  
26 Thermophilic carboxydrotrophs *M. thermoacetica* and *C. hydrogenoformans* lack the RnF-

1 complex and employ energy converting hydrogenases (Ech) in order to generate a cation  
2 gradient and produce ATP (Schuchmann and Müller, 2014; Wu et al., 2005). Although a  
3 CODH-hydrogenase like gene-cluster is found in the genome of ANCO1 (**Figure 4**), the  
4 absence of clear hydrogen production suggests it is not employing it. In addition, this cluster  
5 does not show the typical Ech structure, indicating that in contrast to other CO-utilizing  
6 thermophiles, ANCO1 uses the Rnf-complex for its energy metabolism.

7 Despite the presence of soluble hydrogenases encoded in the genome, strain ANCO1  
8 was unable to grow acetogenically on H<sub>2</sub>/CO<sub>2</sub> or use H<sub>2</sub> as electron donor for anoxic  
9 respiration. The strain did produce minor amounts of H<sub>2</sub> when grown on pyruvate. This raises  
10 the question why strain ANCO1 is able to use CO but not H<sub>2</sub> to drive acetogenesis. A possible  
11 reason are the thermodynamic constrains imposed during H<sub>2</sub>-dependent acetogenesis – the  
12 fact that the standard redox potential of the pair 2H<sup>+</sup>+2e<sup>-</sup>/H<sub>2</sub> (≈-400 mV) is not sufficiently  
13 negative to reduce ferredoxin, demands for bifurcation mechanisms to perform CO<sub>2</sub> reduction  
14 in the WLP (Schuchmann & Müller, 2012; Buckel & Thauer, 2013). Utilization of CO (with a  
15 substantially lower standard redox potential, i.e. E<sup>0'</sup> (CO<sub>2</sub>/CO) ≈ -520 mV) circumvents this  
16 bottleneck, and ferredoxin can be directly reduced via CODH. If ANCO1 is unable to link H<sub>2</sub>-  
17 oxidation to ferredoxin reduction via a bifurcating hydrogenase, this would explain the  
18 absence of acetogenic growth with H<sub>2</sub>/CO<sub>2</sub>. The H<sub>2</sub> that is produced during growth on  
19 pyruvate might originate from Fe-only hydrogenases using ferredoxin as donor, and favouring  
20 the hydrogen producing reaction direction (ref Adams 1990).

21 As ANCO1 encodes for a HDCR-like complex (ACONDI 00243-00246 and 02919-  
22 02924), the WLP appears to be H<sub>2</sub>-dependent in this strain. Hydrogen production via Fe-only  
23 hydrogenases with ferredoxin (derived from CO oxidation) might play a role in introducing  
24 the reduction equivalents via the HDCR-like complex into the WLP. Such internal cycling of  
25 hydrogen by acetogens has been observed before from organic substrates such as fructose

1 (ref. Wiechmann 2020). To note that activity of HDCR-like complex in ANCO1 was not  
2 confirmed experimentally in this study, it is also possible that formate alternatively originates  
3 from bifurcating cytoplasmic enzymes that require NAD(P)H and ferredoxin, similar to what  
4 is observed in *Clostridium autoethanogenum* (wang et al., 2013). In this case, H<sub>2</sub> would not  
5 be required to drive the WLP, allowing operation on CO without intermediate H<sub>2</sub> production.  
6 The potential roles for hydrogenases and their role in acetogenesis are depicted in figure 4  
7 (dotted red lines). Overall, with current information, we can only speculate on the H<sub>2</sub>  
8 metabolism of strain ANCO1 and more biochemical research is required to further elucidate  
9 this.

10       Regarding anaerobic respiration, the ability to utilize fumarate and thiosulfate as the  
11 electron acceptors is reported for *Natranaerobius thermophilus* and *Natranaerobaculum*  
12 *magadiense*, although succinate formation from fumarate was not measured. But the genome  
13 of *N. thermophilus* does contain the genes coding for fumarate reductase and thiosulfate  
14 reductase (Nther\_2664-2665 and Nther\_0643-0644, respectively) with the highest similarity  
15 to the ones present in ANCO1 genome. What is questionable, however, is the universal ability  
16 for the DNRA in the whole "Natranaerobiiia" members described previously. The reasons for  
17 doubts are the following: i) formation of ammonia as the final product was not analyzed in  
18 *Natranaerobius truperii* and *Natronovirga*, and ii) genes encoding for respiratory nitrate  
19 reductases (Nar/Nap) and the NrfAH-type multiheme cytochromes *c* are not present in the  
20 genomes of both *Natranaerobius* species (genomes of *Natronovirga* and *Natranaerobaculum*  
21 are not available). Therefore, this important mode of anaerobic respiration currently can not  
22 be assumed as a common trait? in this group. It is also questionable that as much as 20 mM  
23 nitrate was used in the tests with the "Natranaerobiiia" members. Our experience with  
24 ANCO1 showed, that the complete ammonification is inhibited at far lower nitrate  
25 concentrations. Furthermore, the inability of ANCO1 to directly utilize nitrite for DNRA is

1 also intriguing, pointing out that there is a problem. The root of this "sluggishness" might lay  
2 in the unusual modularity of the DNRA system in this Gram-positive bacterium. The classical  
3 ammonifying nitrite reductase consists of the periplasmic catalytic pentaheme *c* NrfA and its  
4 electron donor tetraheme *c* NrfH, which is an integral membrane quinol-dehydrogenase  
5 (Simon and Klotz, 2013). In ANCO1, only the NrfA subunit is present, which is also a part of  
6 a locus containing a truncated Nap nitrate reductase lacking its cytochrome *c* containing  
7 electron donating NapB and NapC. Such deviations from the classical structures might be  
8 related to the facts that i) ANCO1 does not have a periplasm, and ii) that it does not have the  
9 respiratory quinones, which normally serve as the immediate electron donors for the  
10 periplasmically located respiratory complexes. Therefore, the only available low-redox  
11 potential electron donors in ANCO1 appears to be produced in the cytoplasm [ferredoxins and  
12 NAD(P)H]. This could explain the difficulties with the DNRA growth we observed in  
13 ANCO1, particularly that the nitrite reduction was only possible after initiation of growth  
14 either by pyruvate fermentation or at fumarate-reducing conditions. This might have been  
15 necessary to built up the required low redox potential electron donor pool for nitrate/nitrite  
16 reduction. Regarding the ability for DNRA reported previously in the H<sub>2</sub>/CO-utilizing  
17 acetogens (REFS), it looks like that this is rather complex. At least in two documented cases  
18 (*Moorella thermoacetica* and *Clostridium ljungdahlii*) the ammonification of nitrate/nitrite  
19 does happen, however, no evidence for genes encoding multicytochrome *c* type of  
20 ammonifying Nir (NrfA) are present in the genomes. Instead, the cytoplasmic assimilatory  
21 NADH-dependent NirB seems to operate as the electron sink rather resembling "dump of  
22 electrons" in fermentative prokaryotes (Emerson et al., 2018; Pierce et al., 2008; Seifritz et al.,  
23 2003). Therefore, such process is fundamentally different from the respiratory DNRA.

24

## 25 **Taxonomy**

1 Based on the phylogenomic analysis and unique phenotypic properties we suggest to classify  
2 strain ANCO1 into a new genus and species *Natranaerofaba carboxydovora*, which forms a  
3 new family *Natranaerofabaceae* within the class "*Natranarobiia*".

4

5 ***Natranaerofabaceae* fam. nov.**

6 *Natr.an.ae.ro.fa.ba.ce'ae*. N.L. fem. n. *Natranaerofaba* a bacterial genus; *-aceae* ending to  
7 denote a family; N.L. fem. pl. n. *Natranaerofabaceae*, the family of *Natranaerofaba*.

8

9 The family includes obligately anaerobic, acetogenic, extremely haloalkaliphilic bacteria  
10 living in hypersaline soda lakes. It is a member of class "*Natranarobiia*", phylum *Firmicutes*.

11 The family consists of a single genus and species *Natranaerofaba carboxydovora*. The type  
12 genus is *Natranaerofaba*.

13 ***Natranaerofaba* gen. nov.**

14 *Natr.an.ae.ro.fa'ba* N.L. neut. n. *natron*, derived from Arabic *natrun* soda (sodium carbonate);  
15 Gr. pref. *an-*, not; Gr. masc. n. *aer*, air; L. fem. n. *faba*, bean; N.L. fem. n. *Natranaerofaba*,  
16 bean-shaped soda loving anaerobe.

17

18 The genus includes obligately anaerobic acetogenic bacteria with bean-shaped cells. The polar  
19 lipids are dominated by diethers with phosphocholine and phosphoglycerol polar heads. They  
20 are extremely halophilic and obligately alkaliphilic moderate thermophiles capable of  
21 anaerobic respiration. They can utilize CO and pyruvate during acetogenic growth and  
22 formate and lactate in presence of thiosulfate, fumarate or nitrate as electron acceptors. Form  
23 a deep-branching lineage within the class "*Natranarobiia*", phylum *Firmicutes*. The type  
24 species is *Natranaerofaba carboxydovora*. Family classification: *Natranaerofabaceae*.

25

26 ***Natranaerofaba carboxydovora* sp. nov.**

27

28 *car.bo.xy.do.vo'ra* L. pref. *carboxydum*, carbon monoxide; L. v. *voro*, to devour, consume; L.  
29 fem. adj. *carboxydovora*, consuming carbon monoxide

30

31 Cells possess a Gram-positive type of cell wall and are bean-shaped rods, 0.4 x 3-6  $\mu\text{m}$ ,  
32 motile by peritrichous flagella. Endospore formation is not observed, but the potential is  
33 present in the genome. Polar lipids include phosphocholines and phosphoglycerols, with the  
34 most common core components being mostly present as ether-bound C<sub>14:0</sub> and plasmalogen-  
35 derived aiC<sub>17:0</sub>. Respiratory lipoquinones are not present. The species is strictly anaerobic and  
36 heterotrophic acetogen capable of anaerobic respiration. Acetogenic growth is possible with

1 pyruvate and CO as the electron donors with production of acetate/lactate and acetate/formate  
2 as products, respectively. Anaerobic respiration is possible with CO, pyruvate, formate and  
3 lactate as donors and fumarate and thiosulfate (2-electron reduction) as the electron acceptors.  
4 Lactate is converted to acetate. Formate also supports anaerobic growth with nitrate as  
5 acceptor resulting in formation of ammonia. Yeast extract is utilized as a C-source. Obligately  
6 alkaliphilic with a pH range for growth between 9 and 10.5 and an optimum at pH 9.5-9.7.  
7 Extremely salt-tolerant with a total Na<sup>+</sup> range for growth from 2.5 to 4.5 M (optimum 3.5-4  
8 M). Moderately thermophilic with a temperature range of 35-56 °C and an optimum at 48-50  
9 °C. The type strain was obtained from anaerobic sediments of a hypersaline soda lake in  
10 Kulunda Steppe (Altai region, Russia). DNA G+C is 35.3 mol % (genome). Type strain is  
11 ANCO1<sup>T</sup> (DSM 24608). The EMBL/GenBank genome accession number is CP054394.

12

## 13 **Experimental procedures**

14

15

### 16 **Cultivation conditions**

17 The basic medium used for enrichment and routine cultivation of pure culture was obtained by 1:1  
18 mixing of a NaCl and a sodium carbonate bases both containing 4 M total Na<sup>+</sup> and sterilized separately  
19 at 120°C for 40 min. The NaCl base contained (g/l): NaCl 240, KCl 5, K<sub>2</sub>HPO<sub>4</sub> 2.5, NH<sub>4</sub>Cl 0.5. The  
20 pH was adjusted to 7 by titration with 10% KHPO<sub>4</sub> before sterilization. The carbonate base contained  
21 (g/l): Na<sub>2</sub>CO<sub>3</sub> 190, NaHCO<sub>3</sub> 30, NaCl 16, K<sub>2</sub>HPO<sub>4</sub> 1 (pH 10). After sterilization, both bases were  
22 supplemented with 1 ml/l each of filter-sterilized vitamin and acidic trace metal stock solutions  
23 (Pfennig and Lippert, 1966), 1 ml/l of filter-sterilized alkaline W-Se solution (Plugge, 2007) and 1  
24 mM MgSO<sub>4</sub>. The alkaline base was also supplemented with 4 mM NH<sub>4</sub>Cl from 2 M sterile stock  
25 solution. Finally, the two bases were mixed 1:1 in a sterilized flask, resulting in a 4 M Na<sup>+</sup> Cl-  
26 carbonate alkaline medium with a final of pH 9.7. For enrichment of the potential CO-dependent  
27 methyl-reducing methanogens, this medium was amended with 50 mM MeOH, 2 mM sodium acetate,  
28 100 mg/l yeast extract and 1% (v/v) of autoclaved 1:1 sediment:brine suspension from Bitter-1 soda  
29 lake (according to Sorokin et al., 2017). 40 ml complete medium was dispensed into 115 ml serum  
30 bottles, supplemented with 0.5 mM of sodium filter-sterilized Na<sub>2</sub>S, closed with butyl rubber stoppers  
31 and made anoxic by three cycles of vacuum boiling/sterile argon flushing. Finally, the medium was

1 reduced by adding 20  $\mu$ l of sterile dithionite solution in 1 M sodium bicarbonate. Sterile CO gas was  
2 added at 5-50% in the gas phase on the top of argon. The bottles were inoculated with 1 cm<sup>3</sup> of 1:1  
3 sediment-brine suspension and incubated statically with periodic hand shaking at 50°C.

4 Cultivation of pure culture was mostly done with the same basic medium, whereby CO and  
5 MeOH were replaced by various electron donors with or without electron acceptors. Tests for the Cl<sup>-</sup>  
6 dependence was done by either decreasing the proportion of NaCl base to 0, or increasing it up to a  
7 maximum of 3.9 M (retaining carbonates at a minimal concentration which allowed sufficient  
8 alkalinity for growth). Test for total Na<sup>+</sup> range for growth was done using 1:1 mixture (based of Na<sup>+</sup>  
9 molarity) of NaCl/Na-carbonates, creating a range from 1 to 4.5 M Na<sup>+</sup> at pH 9.5. The pH range for  
10 growth was tested in 3 buffer systems containing 4 M total Na<sup>+</sup>: for the pH from 7 to 8, 50 mM  
11 HEPES-50 mM K<sub>2</sub>HPO<sub>4</sub>/4 M NaCl; for the pH 8-8.5, 4 M NaCl/0.5 M filter-sterilized NaHCO<sub>3</sub>; for  
12 the pH 9-11, 2 M NaCl/2 M Na-carbonate buffer with different proportions of bicarbonate and  
13 carbonate.

#### 15 **Analyses**

16 CO, CO<sub>2</sub>, CH<sub>4</sub> and H<sub>2</sub> in the gas phase were quantified by the GC equipped with a methanator and  
17 flame ionization and thermal conductivity detectors [Chromateck Crystall 5000 (Ufa, Russia);  
18 column Hayesep 80-100 mesh, 2 m x 3 mm, 40 °C; carrier gas Ar]. Nitrite and sulfide were  
19 quantified by colorimetric methods (Gries-Romijn-van Eck, 1966; Trüper and Schlegel, 1964). Nitrate  
20 was monitored qualitatively using Merck sticks after neutralizing the culture supernatant to pH 7. The  
21 organic acids in the liquid phase were analyzed by HPLC. 0.4 ml cell-free culture supernatant was  
22 added to 0.6 ml 0.05 M H<sub>2</sub>SO<sub>4</sub> solution containing 10 mM DMSO as internal standard. Samples were  
23 run on a Shimadzu iSeries Plus (Kioto, Japan), equipped with a MetaCarb 67H column (Agilent  
24 technologies, Santa Clara, CA), operated either at 30 or 45°C with 0.005 M H<sub>2</sub>SO<sub>4</sub> as eluent at a flow  
25 rate of 0.9 ml/min. Both, a UV and RI detector were used for detection of components. Concentrations  
26 could be accurately determined down to 0.1 mM.

1 Activity of anaerobic carbon monoxide dehydrogenase (CODH) was measured via enzymatic  
2 assays. Cells grown with CO were harvested from a 50 ml late exponential phase culture by  
3 centrifugation in anaerobic chamber, the cell pellet was washed with anoxic 0.8 M NaHCO<sub>3</sub> (pH 8.5),  
4 cooled on ice and resuspended in 0.5 M NaHCO<sub>3</sub> (pH 8.5) containing 2 mM DTT. The cells were  
5 disrupted by sonication with a Bandelin Sonopuls (Berlin, Germany), under anaerobic conditions, and  
6 the resulting cell free extract was transferred to rubber stoppered glass vials and kept on ice.  
7 Enzymatic assays were performed in quartz cuvettes sealed with a rubber stopper. After placing the  
8 rubber stopper, the gas phase was flushed twice with nitrogen to remove oxygen, and a final time with  
9 CO. Cuvettes were filled with 0.9 ml 0.8 M NaHCO<sub>3</sub> via syringe and methyl viologen was added at 10  
10 mM final concentration. Before start of the assay the absorbance in the cuvette was set between 0.1  
11 and 0.3 at 578 nm using drops of 100 mM dithionite. The sample was placed in a pre-heated (50°C)  
12 socket in a U-2010 spectrophotometer (Hitachi, Tokyo, Japan). The reaction was started by adding  
13 100, 50 or 25 µl cell free extract. The CO-dependent methyl viologen reduction activity was measured  
14 at 578 nm, while temperature was kept constant at 50°C. The background activity was determined with  
15 N<sub>2</sub> in the headspace instead of CO. Overall background activity was 10 times lower as measured in the  
16 samples fed with CO and activity ceased fast (<1 min). Protein concentrations in the cell free extract  
17 was analyzed by Roti-Nanoquant protein assay (CarlRoth, Karlsruhe, Germany), according to  
18 manufacturer instructions.

19 For the lipid analyses, the cells of pure culture of strain ANCO1 were grown with pyruvate at  
20 50°C until late exponential phase, harvested by centrifugation, washed once with 2 M NaCl and freeze  
21 dried. The extracts for core lipid analysis were hydrolyzed in HCl/MeOH (1.5 N) by refluxing for 3 h.  
22 The hydrolysate was adjusted with aqueous KOH to pH 5, extracted three times with dichloromethane,  
23 and dried over Na<sub>2</sub>SO<sub>4</sub>. Derivatization of the hydrolyzed extract and its analysis were carried out as  
24 described previously (Bale et al., 2019b). Briefly, core lipid quantification was carried out on an  
25 Agilent Technologies 7890B GC with a silica column (CP Sil-5, 25 × 0.32 mm) using the method  
26 described in Bale et al. (2019b). Compound identification was carried out on an Agilent Technologies  
27 7890A gas chromatograph (GC) coupled to an Agilent Technologies 5975C VL MSD mass  
28 spectrometer (MS), operated at 70 eV, with a mass range  $m/z$  50–800 and a scan rate of 3 scans s<sup>-1</sup>.



1 The column and oven settings were the same as for the quantification GC analysis. Compounds were  
2 identified based on literature data and library mass spectra. Intact polar lipids (IPLs) were extracted  
3 from freeze-dried biomass using a modified Bligh-Dyer procedure and analyzed by Ultra High  
4 Pressure Liquid Chromatography-High Resolution Mass Spectrometry (UHPLC-HRMS) as described  
5 previously (Bale et al., 2019a). The presence of respiratory menaquinones was tested as described  
6 previously (Sorokin et al., 2019).

7 For electron microscopy, cells from 1 ml of pure culture grown with pyruvate were harvested  
8 by centrifugation, washed once and resuspended in 0.2 ml 2 M NaCl, pH 7 and stained for 1 min in  
9 1% (w/v) uranyl acetate. The preparations were examined in JEOL 100 model transmission electron  
10 microscope (Japan).

11

## 12 **Genome sequencing and phylogenomic analysis**

13 Genomic DNA was extracted from cells grown with pyruvate+fumarate using the MasterPure Gram  
14 positive DNA extraction kit (Middleton, Wisconsin, USA), according to manufacturer instructions.  
15 Genomic DNA was commercially sequenced at Novogene (Beijing, China) using the PacBio  
16 technology. Genome was assembled using Flye (version 2.7.1) and checked for completeness and  
17 contamination using CheckM (version 1.1.2). The assembled genome was annotated using Prokka  
18 (version 1.14.0). The genome was deposited in the GenBank under accession number CP054394. The  
19 identity of selected functional proteins (including mostly catabolic and pH-salt homeostasis functions,  
20 see **Supplementary Table S1**) from the automatic annotation was verified by using manual Blast in  
21 UniProt.

22 For 16S rRNA gene-based phylogeny, sequences were aligned using MAFFT v7.427 (G-INS-i  
23 strategy) (Nakamura et al., 2018). For phylogenomic analysis the list of 120 bacterial core genes was  
24 taken from Genome Taxonomy DataBase (GTDB) (Parks et al., 2018). These marker genes were  
25 identified in selected genomes, aligned and concatenated using GTDBtk v1.2.0 (Chaumeil et al.,  
26 2019). Alignment was automatically trimmed using trimAl 1.2rev59 by using automated1 and gt 0.95  
27 options (Capella-Gutiérrez et al., 2009). The resulting alignment consisted of 21189 amino acid  
28 residues. In both cases phylogenetic tree was built using IQ-TREE 1.6.12 program (Nguyen et al.,

1 2015) with SH-aLRT test (Anisimova et al., 2011) as well as ultrafast bootstrap with 1000 replicates  
2 (Hoang et al., 2018) and ModelFinder to determine the best-fit model (Kalyaanamoorthy et al., 2017).

3

#### 4 **Proteomic analysis**

5 For the shot-gun proteomic analysis, strain ANCO1 was grown either with pyruvate or CO as the  
6 electron donors and yeast extract as the C-source. 20 mg pelleted cell biomass each (wet weight) were  
7 lysed using B-PER reagent/TEAB buffer and bead beating followed by centrifugation at 14,000 x g  
8 under cooling to collect protein supernatant. The proteins were precipitated with TCA (20% v/v final)  
9 at 4°C followed by washing twice using ice cold acetone. The protein pellet was redissolved in 200  
10 mM ammonium bicarbonate containing 6 M urea, reduced in a 10 mM dithiothreitol solution and  
11 further alkylated using 20 mM iodoacetamide. The solution was diluted to below 1 M urea and  
12 digested using Trypsin at a ratio protease to protein of 1:50. Before analysis, peptides were desalted  
13 using an Oasis HLB solid phase extraction sorbent (Waters) according to the manufacturer protocols.  
14 An aliquot corresponding to approx. 100 ng protein digest was analysed in duplicates using an one  
15 dimensional shot-gun proteomics approach (Köcher et al., 2012). For this, 1 µL of samples were  
16 analysed using a nano-liquid-chromatography system consisting of an ESAY nano LC 1200, equipped  
17 with an Acclaim PepMap RSLC RP C18 separation column (50 µm x 150 mm, 2µm), and an QE plus  
18 Orbitrap mass spectrometer (Thermo). The flow rate was maintained at 300 nL min<sup>-1</sup> over a linear  
19 gradient from 5% to 30% solvent B over 90 min, and finally to 75% B over 25 min. Solvent A was  
20 H<sub>2</sub>O containing 0.1% formic acid, and solvent B consisted of 80% acetonitrile in H<sub>2</sub>O and 0.1%  
21 formic acid. The Orbitrap was operated in data-dependent acquisition mode acquiring peptide signals  
22 from *m/z* 350 -1400, where the top 10 signals were isolated at a window of *m/z* 2.0 and fragmented  
23 using an NCE of 30. The collected data were analysed against the established proteome database,  
24 using PEAKS Studio 8.5 (Bioinformatics Solutions Inc) allowing 20 ppm parent ion mass error  
25 tolerance, 3 missed cleavages, carbamidomethylation as fixed and methionine oxidation and N/Q  
26 deamidation as variable modifications. Peptide spectrum matches were filtered against 1% false  
27 discovery rate (FDR) and protein identifications were accepted as being significant when having 2  
28 unique peptides minimum. Relative protein abundances were correlated to protein molecular weight

1 normalized spectral counts (Hongbin et al., 2004; Keiji and Itoh, 2008). The obtained dataset was  
2 deposited at the proteomics identification database (PRIDE Archive) and are openly available through  
3 the proteome exchange server (<http://www.proteomexchange.org/>, PXD020223;  
4 <http://www.ebi.ac.uk/pride>, reviewer account details: [reviewer26358@ebi.ac.uk](mailto:reviewer26358@ebi.ac.uk)/phJgNecx).

5

6

## 7 **Funding**

8 DYS, MP, MD, DZS, and JSSD acknowledge support from the SIAM-Gravitation Program of the  
9 Dutch Ministry of Education, Culture and Science (24002002). DYS was also supported by the  
10 Russian Foundation of Basic Research (19-04-00401). AM was supported by the Russian Science  
11 Foundation (17-74-30025). NB and JSSD were supported by the European Research Council  
12 (ERC) under the European Union's Horizon 2020 research and innovation programme (grant  
13 agreement No 694569).

14

15

## 16 **Conflict of interests**

17 The authors declare no conflict of interests

18

19

## 20 **References**

21

22 Adams, M. (1990) Structure and mechanism of iron-only hydrogenases. *Biochim Biophys Acta* **1020**:  
23 115-145.

24 Allen, T.D., Caldwell, M.E., Lawson, P.A., Huhnke, R.L., and Tanner, R.S. (2010) *Alkalibaculum*  
25 *bacchi* gen.nov., sp.nov., a CO-oxidizing, ethanol-producing acetogen isolated from livestock-  
26 impacted soil. *Int J Syst Evol Microbiol* **60**: 2483–2489.

27 Angelidis, A.S., and Smith G.M. (2003) Three transporters mediate uptake of glycine betaine and  
28 carnitine by *Listeria monocytogenes* in response to hyperosmotic stress. *Appl. Environ Microbiol*  
29 **69**:1013-1022.

30 Anisimova, M., Gil, M., Dufayard, J.F., Dessimoz, C., and Gascuel, O. (2011) Survey of branch  
31 support methods demonstrates accuracy, power, and robustness of fast likelihood-based  
32 approximation schemes. *Syst Biol* **60**: 685-699.

33 Bale, N.J., Sorokin, D.Y., Hopmans, E.C., Koenen, M., Rijpstra, W.I.C., Villanueva, L., *et al.* (2019a)  
34 New insights into the polar lipid composition of extremely halo(alkali)philic euryarchaea from  
35 hypersaline lakes. *Front Microbiol* **10**: 377.

36 Bale, N.J., Rijpstra, W.I.C., Oshkin, I.Y., Belova, S.E., Dedysh, S.N. and Sinninghe Damsté,  
37 J.S. (2019b) Fatty acid and hopanoid adaption to cold in the methanotroph *Methylovulum*  
38 *psychrotolerans*. *Front Microbiol* **10**: 589.

39 Baudrand, M., Grossi, V., Pancost, R., and Aloisi, G. (2010) Non-isoprenoid macrocyclic glycerol

- 1 diethers associated with authigenic carbonates. *Org Geochem* **41**: 1341–1344.
- 2 Blumenberg, M., Seifert, R., Petersen, S., and Michaelis, W. (2007) Biosignatures present in a  
3 hydrothermal massive sulfide from the Mid-Atlantic Ridge. *Geobiology* **5**: 435–450.
- 4 Buckel, W. (2001) Sodium ion-translocating decarboxylases. *Biochim Biophys Acta* **1527**: 15-25.
- 5 Buckel, W. and Thauer, R.K. (2013) Energy conservation via electron bifurcating ferredoxin reduction  
6 and proton/Na<sup>+</sup> translocating ferredoxin oxidation. *Biochim., Biophys., Acta* **1827**: 94-113.
- 7 Capella-Gutiérrez, S., Silla-Martínez, J.M., and Gabaldón, T. (2009) trimAl: a tool for automated  
8 alignment trimming in large-scale phylogenetic analyses. *Bioinformatics* **25**: 1972–1973.
- 9 Chaumeil, P.A., Mussig, A.J., Hugenholtz, P., Parks, D.H. (2019) GTDB-Tk: a toolkit to classify  
10 genomes with the Genome Taxonomy Database. *Bioinformatics* **36**:1525-1527.
- 11 Devreese, B., Costa, C., Demol, H., Papaefthymiou, V., Moura, I., Moura, J.J.G., et al. (1997) The  
12 primary structure of the split-Soret cytochrome *c* from *Desulfovibrio desulfuricans* ATCC 27774  
13 reveals an unusual type of diheme cytochrome *c*. *Eur J Biochem* **248**: 445-451.
- 14 Dimroth, P., and Schink, B. (1998) Energy conservation in the decarboxylation of dicarboxylic acids  
15 by fermenting bacteria. *Arch Microbiol* **170**: 69-77.
- 16 Drake, H.L., and Daniel, S.L. (2004) Physiology of the thermophilic acetogen *Moorella*  
17 *thermoacetica*. *Res Microbiol* **155**: 869-883.
- 18 Emerson, D.F., Woolston, B.M., Liu, N., Donnelly, M., Currie, D.H., and Stephanopoulos G. (2018)  
19 Enhancing hydrogen-dependent growth of and carbon dioxide fixation by *Clostridium*  
20 *ljungdahlii* through nitrate supplementation. *Biotechnol Bioengineer* **116**: 294-306.
- 21 Fox-Powell M.G., Hallsworth J.E., Cousins C.R., and Cockell C.S. (2016) Ionic strength is a barrier to  
22 the habitability of Mars. *Astrobiology* **16**:427-442.
- 23 Gries-Romijn-van Eck (1966) Physiological and chemical test for drinking water. *NEN 1056, IY-2*  
24 *Nederlandse Normalisatie Instituut Rijswijk*.
- 25 Grossi, V., Mollex, D., Vinçon-Laugier, A., Hakil, F., Pacton, M., and Cravo-Laureau C. (2015)  
26 Mono- and dialkyl glycerol ether lipids in anaerobic bacteria: biosynthetic insights from the  
27 mesophilic sulfate reducer *Desulfatibacillum alkenivorans* PF2803T. *Appl Environ Microbiol* **81**:  
28 3157–3168.
- 29 Hamilton-Brehm, S.D., Gibson, R.A., Green, S.J., Hopmans, E.C., Schouten, S., van der Meer, M.T.J.,  
30 *et al.* (2013) *Thermodesulfobacterium geofontis* sp. nov., a hyperthermophilic, sulfate-reducing  
31 bacterium isolated from Obsidian Pool, Yellowstone National Park. *Extremophiles* **17**: 251-263.
- 32 Henstra, A.M., Dijkema, C., and Stams, A.J. (2007) *Archaeoglobus fulgidus* couples CO oxidation to  
33 sulfate reduction and acetogenesis with transient formate accumulation. *Environ Microbiol* **9**:  
34 1836–1841.
- 35 Herschy, B., Whicher, A., Camprubi, E., Watson, C., Dartnell, L., Ward J., *et al.* (2014) An origin-of-  
36 life reactor to simulate alkaline hydrothermal vents. *J Mol Evol* **79**: 213-227.
- 37 Hoang, D.T., Chernomor, O., von Haeseler, A., Minh, B.Q., Vinh, L.S. (2018) UFBoot2: Improving

- 1 the ultrafast bootstrap approximation. *Mol Biol Evol.* **35**: 518–522.
- 2 Hoefft, S.E., Switzer, Blum J., Stolz, J.F., Tabita, F.R., Witte, B., King, G. M., *et al.* (2007)
- 3 *Alkalilimnicola ehrlichii* sp. nov., a novel arsenite-oxidizing, haloalkaliphilic
- 4 gammaproteobacterium capable of chemoautotrophic or heterotrophic growth with nitrate or
- 5 oxygen as the electron acceptor. *Int J Syst Evol Microbiol* **57**: 504–512.
- 6 Hongbin, L., Sadygov, R.G., and Yates, J.R. (2004) A model for random sampling and estimation of
- 7 relative protein abundance in shotgun proteomics. *Anal Chem* **76**: 4193-4201.
- 8 Huber, R., Wilharm, T., Huber, D., Trincone, A., Burggraf, S., König, H., *et al.* (1992) *Aquifex*
- 9 *pyrophilus* gen. nov. sp. nov., represents a novel group of marine hyperthermophilic hydrogen-
- 10 oxidizing bacteria. *Syst Appl Microbiol* **15**: 340-351.
- 11 Kalyaanamoorthy, S., Minh, B.Q., Wong, T.K.F., von Haeseler, A., Jermin, L.S. (2017) ModelFinder:
- 12 fast model selection for accurate phylogenetic estimates. *Nat Methods* **14**: 587-589.
- 13 Keiji, K., and Itoh, T. (2008) Mass spectrometry-based approaches toward absolute quantitative
- 14 proteomics. *Curr Genom* **9**: 263-274.
- 15 Kempe, S. and Kazmierczak J. (2002) Biogenesis and early life on Earth and Europa: favored by an
- 16 alkaline ocean? *Astrobiology* **2**:123-130.
- 17 King, G.M. (2015). Carbon monoxide as a metabolic energy source for extremely halophilic microbes:
- 18 Implications for microbial activity in Mars regolith. *Proc Nat Ac USA (PNAS)* **112**: 4465-4470.
- 19 Koga, Y., Morii, H., Akagawa-Matsushita, M., and Ohga, M. (1998) Correlation of polar lipid
- 20 composition with 16S rRNA phylogeny in methanogens. Further analysis of lipid component
- 21 parts. *Biosc Biotechnol Biochem* **62**: 230-236.
- 22 Köcher, T., Pichler, P., Swart, R., and Mechtler, K. (2012) Analysis of protein mixtures from whole-
- 23 cell extracts by single-run nanoLC-MS/MS using ultralong gradients. *Nat Protocols* **7**: 882.
- 24 Langworthy, TA, Holzer, G, Zeikus, J.G., and Tornabene T.G. (1983) Iso- and anteiso-branched
- 25 glycerol diethers of the thermophilic anaerobe *Thermodesulfotobacterium commune*. *Syst Appl*
- 26 *Microbiol* **4**: 1-17.
- 27 Liu, K., Atiyeh, H.K., Tanner, R.S., Wilkins, M.R., and Huhnke R.L. (2012) Fermentative production
- 28 of ethanol from syngas using moderately alkaliphilic strains of *Alkalibaculum bacchi*. *Bioresour*
- 29 *Technol* **104** 336–341.
- 30 Mesbah, N.M., Hedrick, D.B., Peacock, A.D., Rohde, M., and Wiegel J. (2007) *Natronaerobius*
- 31 *thermophilus* gen. nov. sp. nov., a halophilic, alkalithermophilic bacterium from soda lakes of the
- 32 Wadi An Natrun, Egypt, and proposal of *Natronaerobiaceae* fam. nov. and *Natronaerobiales*
- 33 ord. nov. *Int J Syst Evol Microbiol* **57**: 2507–2512.
- 34 Mesbah, N.M., Cook, G.M., and Wiegel, J. (2009) The halophilic alkalithermophile *Natronaerobius*
- 35 *thermophilus* adapts to multiple environmental extremes using a large repertoire of Na<sup>+</sup>(K<sup>+</sup>)/H<sup>+</sup>
- 36 antiporters. *Mol Microbiol* **74**: 270–281.
- 37 Mesbah, N.M., and Wiegel J. (2009) *Natronovirga wadinatrunensis* gen. nov., sp. nov. and

- 1 *Natranaerobius trueperi* sp. nov., halophilic, alkalithermophilic micro-organisms from soda  
2 lakes of the Wadi An Natrun, Egypt. *Int J Syst Evol Microbiol* **59**: 2042–2048.
- 3 Nakamura, T., Yamada, K.D., Tomii, K., and Katoh, K. (2018) Parallelization of MAFFT for large-  
4 -scale multiple sequence alignments. *Bioinformatics*. **34**: 2490–2492.
- 5 Nguyen, L.T., Schmidt, H.A., von Haeseler, A., and Minh, B.Q. (2015) IQ-TREE: a fast and effective  
6 stochastic algorithm for estimating maximum-likelihood phylogenies. *Mol Biol Evol.* **32**: 268–  
7 274.
- 8 Ongagna-Yhombi, S.Y., McDonald, N.D., Boyd E.F. (2015). Deciphering the role of multiple  
9 betaine-carnitine-choline transporters in the halophile *Vibrio parahaemolyticus*. *Appl Environ*  
10 *Microbiol* **81**: 351-363.
- 11 Pancost, R.D., Pressley, S., Coleman, J.M., Talbot, H.M., Kelly, S.P., Farrimond, P., *et al.*  
12 (2006) Composition and implications of diverse lipids in New Zealand Geothermal  
13 sinters. *Geobiology* **4**: 71–92.
- 14 Parks, D.H., Chuvochina, M., Waite, D.W., Rinke, C., Skarshewski, A., Chaumeil, P.-A., *et al.* (2018)  
15 A standardized bacterial taxonomy based on genome phylogeny substantially revises the tree of  
16 life. *Nat Biotechnol* **36**: 996–1004.
- 17 Parshina, S.N., Sipma, J., Henstra, A.M., and Stams, A.J.M. (2010) Carbon monoxide as an electron  
18 donor for the biological reduction of sulphate. *Int J Microbiol* 2010: 319527.
- 19 Pfennig, N., and Lippert, K.D. (1966) Über das Vitamin B12–bedürfnis phototropher Schwefel  
20 Bakterien. *Arch. Microbiol.* **55**: 245–256.
- 21 Pflüger K, Müller V. 2004. Transport of compatible solutes in extremophiles. *J Bioenerg Biomembr*  
22 **36**:17–24
- 23 Pierce, E., Xie, G., Barabote, R.D., Saunders, E., Han, C.S., Detter, J.C., *et al.* (2008) The complete  
24 genome sequence of *Moorella thermoacetica* (f. *Clostridium thermoaceticum*). *Environ*  
25 *Microbiol* **10**: 2550–2573.
- 26 Plugge, C.M. (2005) Anoxic media design, preparation, and considerations. *Methods Enzymol* **397**: 3-  
27 16.
- 28 Rebouche, C.J. (1998). Carnitine metabolism and its regulation in microorganisms and mammals. *Ann*  
29 *Rev Nutr* **18**: 39-61.
- 30 Roberts, M.F. (2005). Organic compatible solutes of halotolerant and halophilic microorganisms.  
31 *Saline Syst* **1**:5.
- 32 Schagerl, M. (ed). (2016) Soda lakes of East Africa. Springer International Publishing AG  
33 Switzerland, pp. 408.
- 34 Schuchmann, K., and Müller, V. (2012) A bacterial electron-bifurcating hydrogenase. *J Biol Chem*  
35 **287**: 31165–31171.
- 36 Schuchmann, K., and Müller, V. (2013) Direct and reversible hydrogenation of CO<sub>2</sub> to formate by a

- 1 bacterial carbon dioxide reductase. *Science* **342**: 1382-1385.
- 2 Schuchmann, K., and Müller, V. (2014) Autotrophy at the thermodynamic limit of life: a model for  
3 energy conservation in acetogenic bacteria. *Nat Rev Microbiol* **12**: 809-821.
- 4 Seifritz, C., Drake, H.L., and Daniel, S.L. (2003) Nitrite as an energy-conserving electron sink for the  
5 acetogenic bacterium *Moorella thermoacetica*. *Curr Microbiol* **46**:329–333.
- 6 Simon, J., and Klotz, M.G. (2013) Diversity and evolution of bioenergetic systems involved in  
7 microbial nitrogen compound transformations. *Biochim Biophys Acta* **1827**: 114–135.
- 8 Sorokin, D.Y. (2017) Anaerobic haloalkaliphiles. In: *Encyclopedia Life Science*. John Wiley & Sons,  
9 Ltd:Chichester. doi: 10.1002/9780470015902.a0027654.
- 10 Sorokin, D.Y., Banciu H.L., and Muyzer, G. (2015) Functional microbiology of soda lakes. *Curr Opin*  
11 *Microbiol* **25**: 88–96.
- 12 Sorokin, D.Y., Makarova, K.S., Abbas, B., Ferrer, M., Golyshev, P.N., Galinski, E.A., *et al.* (2017)  
13 Discovery of extremely halophilic, methyl-reducing euryarchaea provides insights into the  
14 evolutionary origin of methanogenesis. *Nat Microbiol* **2**: 17081.
- 15 Sorokin, D.Y., Merkel, A.Y., Abbas, B., Makarova, K., Rijpstra, W.I.C., Koenen, M., *et al.* (2018)  
16 *Methanonatronarchaeum thermophilum* gen. nov., sp. nov., and '*Candidatus*  
17 *Methanohalarchaeum thermophilum*' - extremely halo(natrono)philic methyl-reducing  
18 methanogens from hypersaline lakes representing a novel euryarchaeal class  
19 *Methanonatronarchaeia* classis nov. *Int J Syst Evol Microbiol* **68**: 2199-2208.
- 20 Sorokin, D.Y., Yakimov, M.M., Messina, E., Merkel, A.Y., Bale, N.J., and Sinninghe Damsté J.S.  
21 (2019) *Natronolimnobius sulfurireducens* sp. nov., and *Halalkaliarchaeum desulfuricum* gen.  
22 nov., sp. nov., the first sulfur-respiring alkaliphilic haloarchaea from hypersaline alkaline lakes.  
23 *Int J Syst Evol Microbiol* **69**: 2662-2673.
- 24 Trüper, H.G., and Schlegel, H.G. (1964) Sulfur metabolism in *Thiorhodaceae*. 1. Quantitative  
25 measurements on growing cells of *Chromatium okenii*. *Antonie van Leeuwenhoek* **30**:  
26 225-238.
- 27 van Dongen, B.E., Roberts, A.P., Schouten, S., Jiang, W.-T., Florindo, F., and Pancost, R.D.  
28 (2007) Formation of iron sulfide nodules during anaerobic oxidation of methane.  
29 *Geochim Cosmochim Acta* **71**: 5155–5167.
- 30 van Gelder, A.H., Sousa, D.Z., Rijpstra, W.I.C., Sinninghe Damsté, J.S., Stams, A.J.M., and Sánchez-  
31 Andrea, I. (2014) *Ercella succinigenes* gen. nov., sp. nov., an anaerobic succinate-producing  
32 bacterium. *Int J Syst Evol Microbiol* **64**: 2449-2454.
- 33 Vavourakis C.D., Andrei, A.S., Mehrshad, M., Ghai, R., Sorokin, D. Y., and Muyzer, G. (2018) A  
34 metagenomics roadmap to the uncultured genome diversity in hypersaline soda lake sediments.  
35 *Microbiome* **6**: 1–18.
- 36 Vavourakis, C. D., Ghai, R., Rodriguez-Valera, F., Sorokin, D. Y., Tringe, S. G., Hugenholtz, P., *et al.*

- 1 (2016) Metagenomic insights into the uncultured diversity and physiology of microbes in four  
2 hypersaline soda lake brines. *Front Microbiol* **7**: 211.
- 3 Wang, S., Huang H., Kahnt, J., Müller A.P., Köpke M., and Thauer R.K. (2013) NADP-specific  
4 electron-bifurcating [fefe]-hydrogenase in a functional complex with formate dehydrogenase in  
5 *Clostridium autoethanogenum* grown on CO. *J Bacteriol* **195**: 4373-4386.
- 6 Weghoff, M.C., Bertsch W.J., and Müller V. (2015) A novel mode of lactate metabolism in strictly  
7 anaerobic bacteria. *Environ. Microbiol* **17**: 670-677.
- 8 Wiechmann, A., Ciurus, S., Oswald F., Seiler, V.N., and Müller, V. (2020) It does not always take  
9 two to tango: “Syntrophy” via hydrogen cycling in one bacterial cell. *ISME J* **14**: 1561-1570.
- 10 Wu, M., Ren, Q., Durkin, A.S, Daugherty, S.C., Brinkac, L.M., Dodson, R.J., *et al.* (2005) Life in hot  
11 carbon monoxide: the complete genome sequence of *Carboxydotherrmus hydrogenoformans* Z-  
12 2901. *PLoS Genetics* **1**: e65.
- 13 Zavarzina, D.G., Zhilina, T.N., Kuznetsov, B.B., Kolganova, T.V., Osipov, G.A., Kotelev, M.S., *et al.*  
14 (2013) *Natranaerobaculum magadiense* gen. nov., sp. nov., an anaerobic, alkalithermophilic  
15 bacterium from soda lake sediment. *Int J Syst Evol Microbiol* **63**: 4456-4461.
- 16 Ziegenbalg, S.B., Birgel, D., Hoffmann-Sell, L., Pierre, C., Rouchy, J.M., Peckmann, J. (2012)  
17 Anaerobic oxidation of methane in hypersaline Messinian environments revealed by <sup>13</sup>C-  
18 depleted molecular fossils. *Chem Geol* **292–293**: 140–148.
- 19 Zorz, J.K., Sharp, C., Kleiner, M., Gordon, P.M.K., Pon, R.T., Dong, X., *et al.* (2019) A shared core  
20 microbiome in soda lakes separated by large distances. *Nat Comm* **10**: 4230.



1 **Table 1.** Utilization of various electron donors/acceptors by strain ANCO1 during  
 2 anaerobic growth at 48°C in a medium containing 4 M total Na<sup>+</sup>, pH 9.7, supplemented  
 3 with 500 mg/l of yeast extract as the carbon source.

<i>e</i> -donor	<i>e</i> -acceptor	Growth	Biomass yield increase (times)*	Products from donor	Products from acceptor
CO	-	+		Acetate/formate	-
	Fumarate	+	1.5	Acetate	Succinate (0.5 mM)
	Thiosulfate	+	1.2	nd	HS <sup>-</sup> (up to 8 mM)
Pyruvate	-	+		Acetate/lactate/H <sub>2</sub>	-
	Fumarate	+	2.2	Acetate/lactate	Succinate 0.5 (mM)
	Thiosulfate	+	1.6	nd	HS <sup>-</sup> (up to 11 mM)
Lactate	-	-			
	Fumarate	w	-	Acetate	Succinate (0.5 mM)
	Thiosulfate	+	-	Acetate	HS <sup>-</sup> (up to 12 mM)
Formate	-	-			
	Fumarate	+	-	CO <sub>2</sub>	Succinate (5.7 mM)
	Thiosulfate	+	-		HS <sup>-</sup> (up to 4 mM)
	Nitrate/nitrite	+	-		NH <sub>3</sub> (up to 5 mM)

4 \*In comparison to growth without acceptor; nd, not determined;

1 **Table 2:** Relative abundance (% of total) of core lipids released after acid  
 2 hydrolysis of cells of ANCO1.

Alkyl carbon number	Alkyl component	Individual %	Carbon number sum %
14	C14:0 FA <sup>1</sup>	1.6	<b>15.5</b>
	C14:0 MGE <sup>2</sup>	<b>13.9</b>	
15	<i>iso</i> C15:0 MGE <sup>2</sup>	0.3	0.5
	C15:0 MGE <sup>2</sup>	0.2	
16	C16:0 FA <sup>1</sup>	2.9	5.8
	C16:0 DA <sup>3</sup>	0.3	
	C16:0 MGE <sup>2</sup>	2.6	
17	10-Me C16:0 FA <sup>1</sup>	3.9	<b>23.3</b>
	<i>iso</i> + <i>anteiso</i> C17:0 DA <sup>3</sup>	<b>17.9</b>	
	<i>iso</i> C17:0 MGE <sup>2</sup>	0.7	
	<i>anteiso</i> C17:0 MGE <sup>2</sup>	0.6	
	C17:0 MGE <sup>2</sup>	0.2	
18	C18:0 FA <sup>1</sup>	2.4	3.1
	C18:0 DA <sup>3</sup>	0.2	
	1-OH C18:0 alcohol	0.5	
19	<i>iso</i> C19:0 FA <sup>1</sup>	0.3	1.4
	<i>iso</i> C19:0 DA <sup>3</sup>	1.1	
Dialkyls	C29:0 DGE <sup>4</sup>	0.5	
	C31:0 DGE <sup>4</sup>	<b>21.1</b>	
	C31:0 Macrocyclic DGE <sup>4</sup>	1.3	
	C32:0 DGE <sup>4</sup>	3.1	
	C33:0 DGE <sup>4</sup>	4.4	
	C34:0 DGE <sup>4</sup>	<b>12.8</b>	

3 Components formed during acid hydrolysis: <sup>1</sup>fatty acid derived from ester-bound alkyl chains;  
 4 <sup>2</sup>monoalkyl glycerol ethers, not including glycerol carbons; <sup>3</sup>dimethyl acetals derived from  
 5 alk-1-enyl ether substituents of plasmalogen lipids; <sup>4</sup>dialkyl glycerol ethers (sum of two  
 6 alkyl chains, not including glycerol carbons). Trace level components ( $\leq 0.1\%$ ) are not given.  
 7

## 1 Legend to the figures

2 **Fig. 1** Cell morphology of strain ANCO1 grown at 4 M total Na<sup>+</sup>, pH 9.7 and 50°C. (**a**, **b**),  
3 phase contrast microphotographs of cells grown with CO and pyruvate, respectively; (**c**)  
4 electron microphotograph of a cell showing flagellation.

5  
6 **Fig. 2** Phylogeny of ANCO1 based on (**a**) 16S rRNA gene sequence analysis and (**b**) the  
7 phylogenomic analysis of 120 bacterial conserved single copy protein coding genes  
8 (taxonomic designations correspond to the Genome Taxonomy Data Base) (Parks et al.,  
9 2018). Only sequences from the type species were used. The trees were built using IQ-TREE  
10 (Nguyen et al., 2015). Bootstrap values above 80% are shown at the nodes. Bar, 0.10 changes  
11 per position.

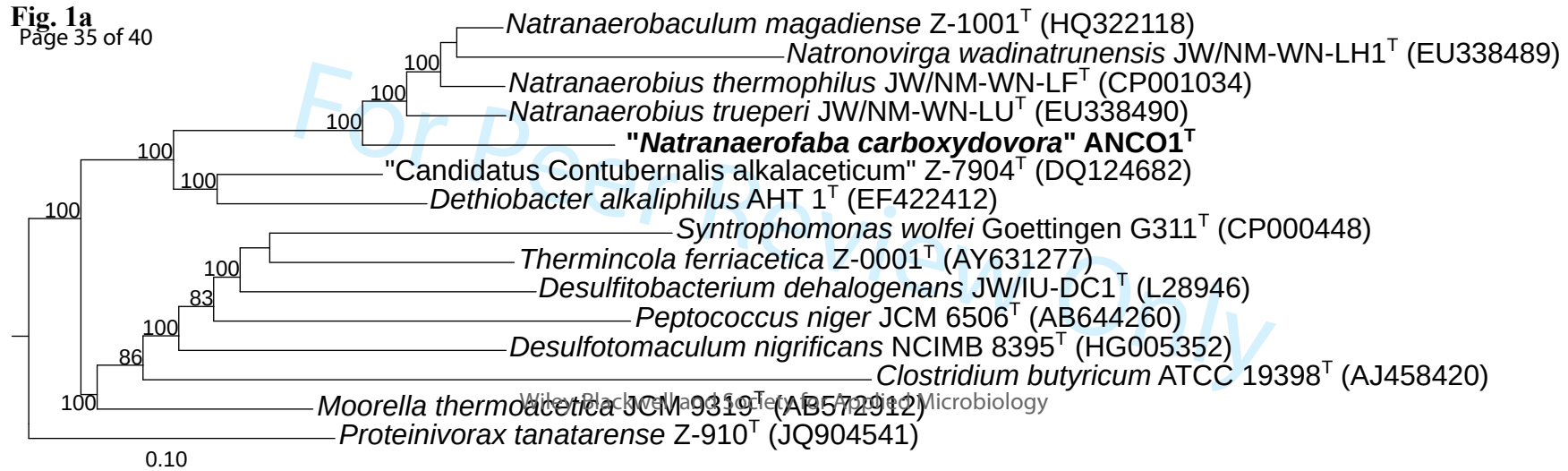
12  
13 **Fig. 3** Influence of pH (at 4 M total Na<sup>+</sup>) (**a**) and salinity (at pH 9.5) (**b**) on growth of strain  
14 ANCO1 with pyruvate+fumarate at 48°C. The data are mean from parallel duplicate cultures.

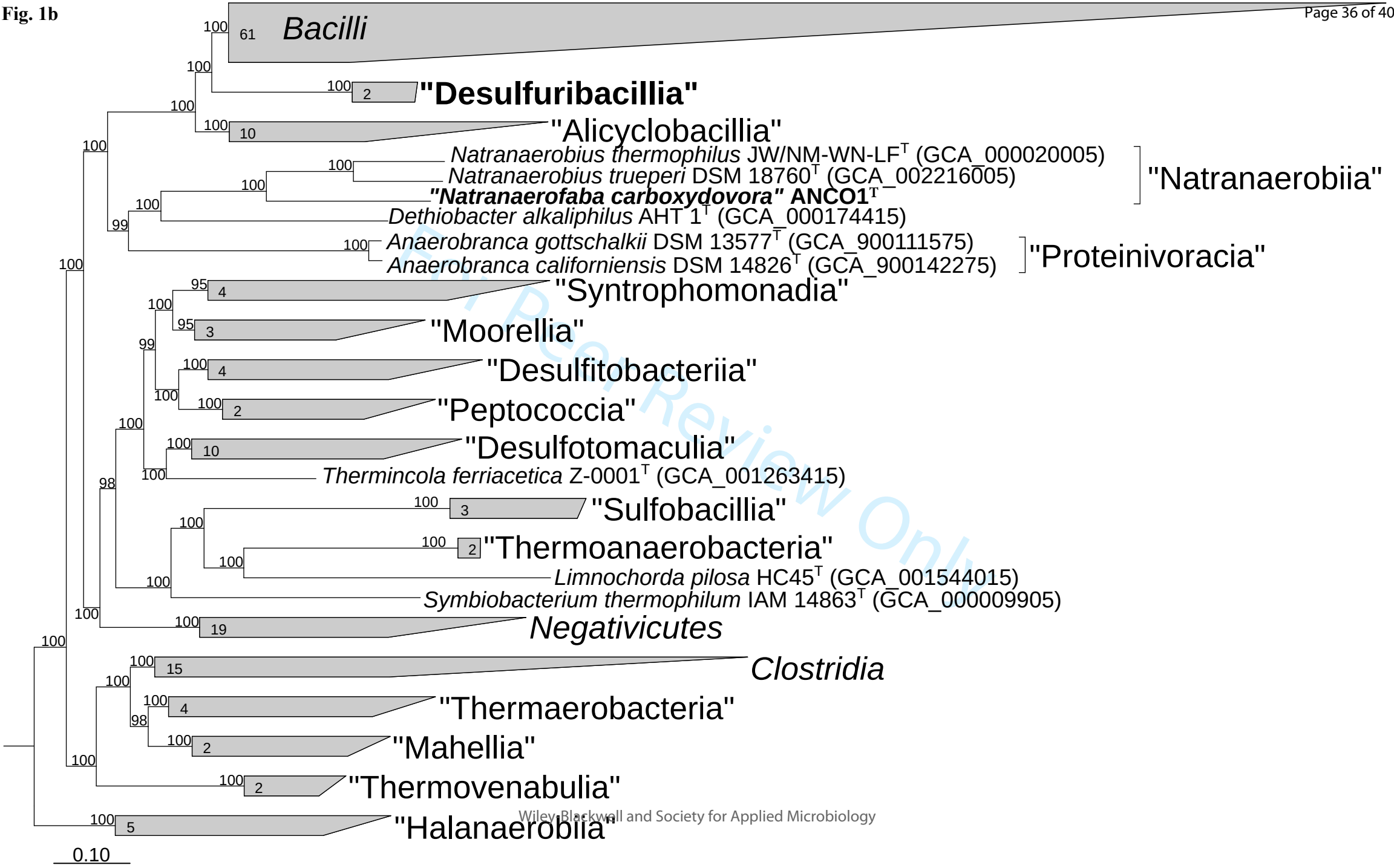
15  
16 **Fig. 4** Overview of the metabolism of ANCO1, including associated locus tags. Dashed lines  
17 represent multiple reactions. Dotted lines represent putative hydrogenase reactions taking  
18 place in the metabolism. Subunits of complexes that are shadowed in grey could not be found.  
19 Colors indicate specific pathways: CO-utilization pathways (red), Rnf-complex & ATP-  
20 synthase (pink), fumarate respiratory complex (green), nitrate respiration complex (blue),  
21 thiosulfate respiration complex (yellow). Abbreviations: CODH: carbon monoxide  
22 dehydrogenase; ACS: acetyl-CoA synthase; fdh/HDRC: formate dehydrogenase; formyl-THF  
23 synthase; metF : methylene-THF reductase; folD: formyl-THF cyclohydrolase/ methylene-  
24 THF dehydrogenase; pta: phospho-acetyltransferase; ack: acetate kinase; acsA: acetyl-CoA  
25 synthase; por: pyruvate oxidoreductase; ppd: phosphopyruvate decarboxylase; pps:  
26 phosphoenolpyruvate synthase; pkn: pyruvate dehydrogenase; me: malic enzyme; fum:  
27 fumarate hydratase; frd: fumarate reductase; sco: succinyl-CoA synthetase; kor: 2-  
28 oxoglutarate oxidoreductase; idh: isocitrate dehydrogenase; aco: cis-aconitase; csy: citrate  
29 synthase; mmd: methylmalonyl-CoA decarboxylase; gcd: glutaconyl-CoA decarboxylase;  
30 mnh: Na<sup>+</sup>/H<sup>+</sup> antiporter; nrfA: nitrite reductase; phs: thiosulfate reductase.

31  
32 **Fig. 5** Organization of the CODH/ acetyl-CoA synthase (ACS) operon in ANCO1 compared  
33 to other carboxydrotrophs. Gene abbreviations: *cooC* : CODH chaperone; *acsA* : CODH

1 ; *acs B*: ACS; *acsC* : corrinoid iron-sulfur protein large subunit; *orf7* : unknown; *acsF*: ACS  
2 chaperone; *acsD* : corrinoid iron-sulfur protein small subunit; *acsE* : methyltransferase  
3 A; *fhs* : formyl-THF synthase; *metF* : methylene-THF reductase; *acoL* : dihydrolipoamide  
4 dehydrogenase; *fold* : formyl-THF cyclohydrolase/methylene-THF dehydrogenase.  
5

For Peer Review Only





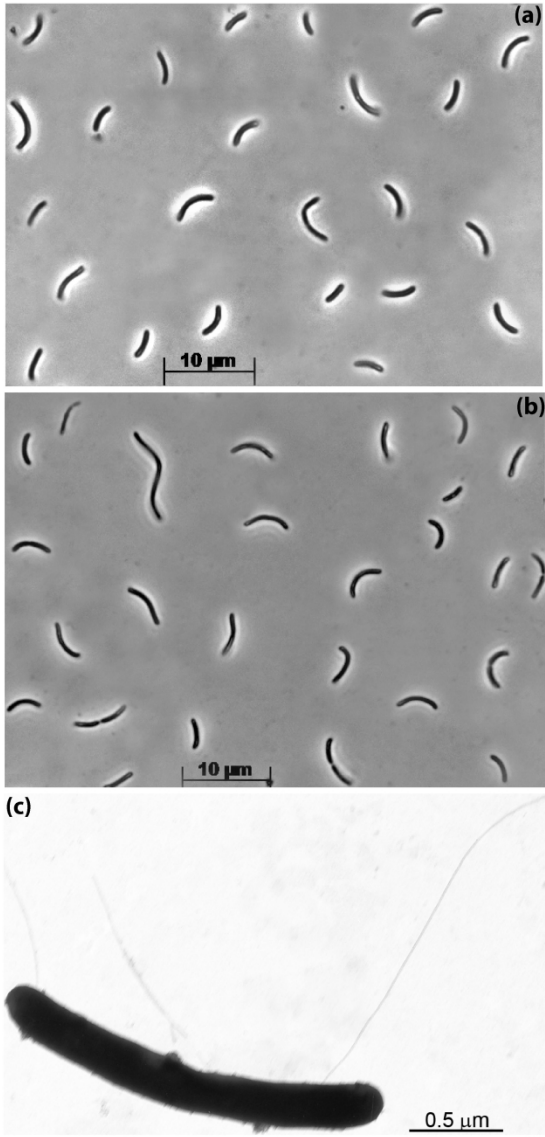


Fig. 2

fig.2

93x206mm (600 x 600 DPI)

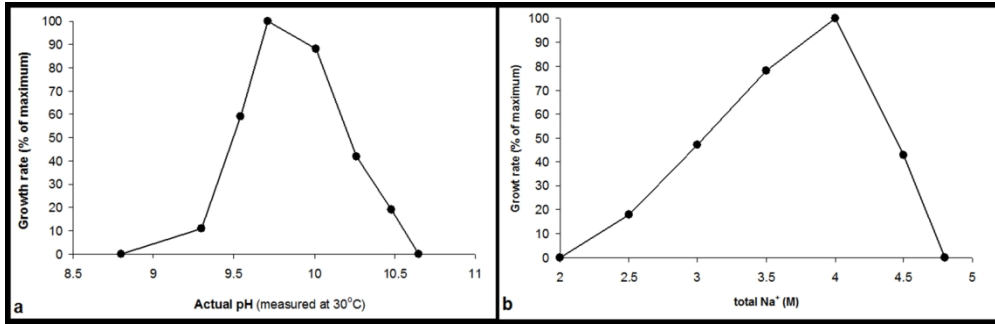


fig.3

237x76mm (300 x 300 DPI)

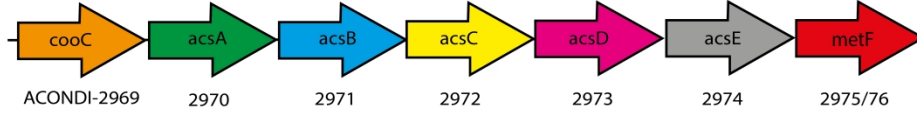


## Unable to Convert Image

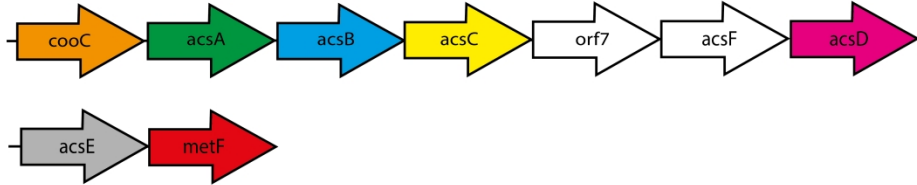
The dimensions of this image (in pixels) are too large to be converted. For this image to convert, the total number of pixels (height x width) must be less than 40,000,000 (40 megapixels).

fig.4\_rev2

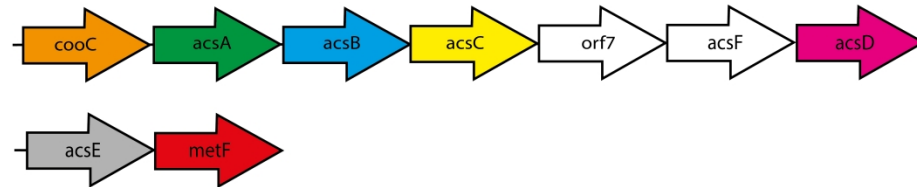
ANCO1



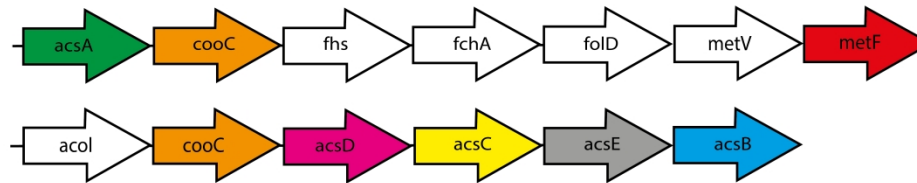
*Moorella thermoacetica*



*Carboxydotherrnus hydrogenoformans*



*Clostridium ljungdahlii*



*Acetobacterium woodii*

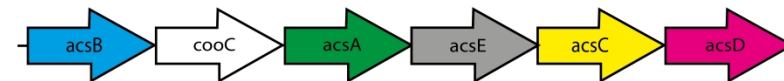


fig.5